2016-01-01

Density Functional Study of Reactivity and Regioselectivity of H2O@C60

Govinda Bahadur Kc
University of Texas at El Paso, gbkc@miners.utep.edu

DENSITY FUNCTIONAL STUDY OF REACTIVITY AND

REGIOSELECTIVITY OF

$H_2O@C_{60}$

GOVINDA BAHADUR KC

Master's Program in Physics

APPROVED:

Rajendra Zope, Ph.D., Chair

Tunna Baruah, Ph.D.

Cristian E. Botez, Ph.D.

Mahesh Narayan, Ph.D.

Jose U. Reveles Ramirez, Ph.D.

Charles Ambler, Ph.D.
Dean of the Graduate School

DENSITY FUNCTIONAL STUDY OF REACTIVITY AND REGIOSELECTIVITY $H_2O@C_{60}$

by

GOVINDA BAHADUR KC

THESIS

Presented to the Faculty of the Graduate School of

The University of Texas at El Paso

in Partial Fulfillment

of the Requirements

for the Degree of

MASTER OF SCIENCE

Department of Physics

THE UNIVERSITY OF TEXAS AT EL PASO

August 2016

Dedication

To my family and friends

Acknowledgements

Any scholarly work is never a result of an individual effort. As a matter of fact, many brains are drained in the production of a single research work. My thesis is not an exception to this rule. Those who provided me with intellectual and emotional support during my research include many, and to acknowledge all of them on this page would be impossible. I hope they will excuse me for using their ideas without particular acknowledgement. However, I must acknowledge some of the scholars without whose scholarly guidance; this research would not have been born.

First of all, I must record my debt to my advisor/supervisor Prof. Dr. Rajendra Zope for his scholarly guidance. In fact, Dr. Zope was always with me encouraging and supporting me whenever I was baffled or confused. He is the one who walked me through the research process—beginning with how to formulate research questions to analyzing, discussing and finding results. Secondly, I would like thank to Dr. Tunna Baruah for her unconditional support and guidance.

I would like to express my special gratitude to Dr. Jose U. Reveles Ramirez for his great support throughout this work. Without help of him, this thesis would not come to this point. I am so grateful with Dr. Luis Basurto, Dr. Yoh Yamamoto, Mr. Shusil Bhusal and all the members of Electronic Structure Lab for helping me in different situations of this research work.

Abstract

The exohedral reactivity of endohedral fullerene has aroused significant interest because of its potential applications in biology, medicine and material science. The encapsulation of a single water molecule without any hydrogen bonding to other compounds, inside the hydrophobic environment of C_{60} is an intriguing topic to study about. In 2011, Kurotobi and Murata were successfully synthesized $H_2O@C_{60}$ fullerene. The presence of a polar water molecule inside the cage is expected to cause changes in the exohedral reactivity of C_{60}. In order to find out the impact of an entrapped single water molecule on the reactivity of C_{60} fullerene, we use density functional theory to study the thermodynamics and kinetics of [4+2] Diels-Alder reaction of 1, 3 cis butadiene at all non-identical bonds of free C_{60} and $H_2O@C_{60}$. Our calculations show that the encapsulation of a single water molecule does not have any significant effect on the exohedral reactivity compared to free C_{60}. Moreover, the obtained reaction energies and activation barriers indicate that [6, 6] bond is more reactive than [5, 6] bond and thus cycloaddition is clearly favored at [6, 6] bond. The dipole moment of the $H_2O@C_{60}$ is only 0.48 Debye significantly smaller than that of water molecule. The infrared and Raman spectra of the endohedral fullerene are also computed.

Table of Contents

List of Tables

List of Figures

Chapter 1: Introduction

Water is an important component in our world and plays a significant role in many biological and chemical fields. It normally exists in hydrogen-bonded environment. A water molecule (H_2O) has a simple structure with two hydrogen atoms bonded to one oxygen atom. The unequal sharing in the O-H bonds result oxygen with a partial negative charge and hydrogen with partial positive charge. The geometry structure of the water molecule and accumulation of charges on two different sides cause the water to be a polar molecule. The water molecules form hydrogen bonds to each other and align based on their polarity. The unique properties of water are based on hydrogen bonding, such as its high boiling and melting points, high dielectric constant, and ability to act as both acid and base. The study of a single water molecule of H_2O without any hydrogen bonding to other compounds is an intriguing topic to study about. [1] The C_{60} fullerene is highly symmetric and nonpolar cage. It is soluble in many nonpolar solvents like carbon disulfide and benzene but it is virtually insoluble in water. The inner space of C_{60} is spherical with radius of 3.7 Å. The entrapment of a water molecule inside the C_{60} fullerene provides an opportunity to study H_2O in a homogenous, highly symmetrical and isolated environment. The encapsulation of a water molecule inside C_{60} ($H_2O@C_{60}$) was first studied experimentally by Kei Kurotobi and Yasujiro Murata in 2011. [2] It was synthesized by molecular surgical approach. The molecular surgical approach refers to the chemical opening of cage, insertion of endohedral unit(s) and the chemical closing of the cage. One of the important characteristics of the properties of H_2O molecule is it has high dipole moment, whereas C_{60} with its high icosahedral symmetry does not have dipole. Thus we expect that $H_20@C_{60}$ is a polar molecule.

Endohedral fullerenes are attributed to encapsulate wide varieties of species, including atoms, molecules, ions or clusters. The physical and chemical properties of the system are mainly controlled by the endohedral units. Because of the potential application in various fields such as biology, medicine, material science, it is extensively studied over the last few years. Although there are many studies have been carried out about the endohedral fullerenes, a current significant topic is the exohedral effect of these compounds. The encapsulated water molecule is expected to modify the exohedral reactivity of $H_2O@C_{60}$ cage with respect to free C_{60}. To the best of our knowledge, the theoretical study on the exohedral reactivity of the $H_2O@C_{60}$ has not done before. The recent study of exohedral reactivity of endohedral compounds is the theoretical study of reactivity and regioselectivity of noble gas endohedral compounds. [3] They analyzed the thermodynamics and the kinetics of [4+2] Diels-Alder cycloaddition of 1, 3-*cis*-butadiene at all nonequivalent bonds in free C_{60}, $Ng@C_{60}$ and $Ng_2@C_{60}$. They found that the effect of noble gas encapsulation inside is not profound compared to free C_{60} which is in agreement with experimental results. However, the exohedral reactivity of endohedral fullerenes encapsulating the heavier noble gas dimers is clearly enhanced. The cycloaddition is favored at [6, 6] bonds in all these cases. Moreover, in the case of $Xe_2@C_{60}$, both [6, 6] and [5, 6] bonds are equally viable. We have studied the [4+2] Diels Alder reaction between 1, 3 cis butadiene and all nonequivalent bonds of a single water molecule endohedral compound $H_2O@C_{60}$ and free C_{60}. Because of high icosahedral symmetry, C_{60} has only two kinds of C-C bonds, which are [6, 6] and [5, 6] or [6, 5] bonds. We searched for the transition states for all the isomers by the method of constrained optimization and calculated the activation barriers.

1.1 Fullerenes

Fullerenes are hollow carbon cages made up of hexagons and pentagons wherein each carbon atom has three-fold coordination. Introduction of a pentagon in a planar hexagonal sheet results in a curvature and using exactly 12 pentagons carbon cage can be made close. The smallest carbon fullerene cage is thus C_{20} with all pentagons and no hexagons. The carbon cages can be obtained by introducing hexagons. For a given carbon cage, depending on the number of atoms, there are several possible ways the hexagonal and pentagonal rings can be arranged. These possibilities increase rapidly with the size of carbon cage, that is, with the number of carbon atoms. The smallest carbon cage in which the pentagonal can be isolated from each other is the C_{60} carbon cage. Such carbon is one of 1812 isomers (number of different arrangements of pentagons and hexagons) of the C_{60} fullerene and has the icosahedral symmetry. This fullerene was first observed in the laboratory by Kroto, Curl and Smalley [4] for which they received Nobel Prize in Chemistry in 1996. In 1991, Huffman, Krätschmer, Lamb, and Fostriopoulos reported a technique to produce gram-sized samples of fullerene powder. These works led to revolution in carbon based nanoscience which established a field of fullerene science which subsequently evolved in studies of carbon nanotubes, graphene etc.

1.2 Endohedral Fullerenes

Endohedral Fullerenes or endo-fullerenes are the carbon cages that are composed of combination of hexagons and pentagons and enclose the extra atoms, molecules, ions or clusters with their inner surfaces. Different isomers can be formed just by varying the positions of hexagons and pentagons. The first synthesized endohedral fullerene was Lanthanum C_{60} ($La@C_{60}$) in 1985. [5] The endohedral unit plays important role for the properties of endohedral fullerene. The endohedral fullerenes can be differentiated as metallo-fullerene, non-metal doped

fullerene and molecular endo-fullerene depending up on the endohedral unit. The properties of fullerene and endohedral fullerene differ each other. The applications of endohedral fullerene are wide and versatile in research fields depending up on the endohedral unit(s). The inner space of the fullerene C_{60} is suitable to enclose the water molecule. The encapsulation of a water molecule inside the fullerene cage was first studied by Kei Kurotobi and Yasujire Murata in 2011 [ ]. The endohedral fullerene $H_2O@C_{60}$ possesses a dipole moment due to the polar nature of the trapped water molecule, altering the inherent physical properties of the empty fullerene C_{60}. For example, the encapsulation of the single water molecule has promoted the solubility of C_{60} in polar solvents. [6]

1.3 C-C bond types

The structure of the fullerene cage has two different bond types; [6, 6] and [5, 6] bonds as it is constituted by hexagonal and pentagonal rings. The bond between two hexagonal rings is [6, 6], whereas the bond between pentagonal and hexagonal rings is [5, 6]. If the type of the rings that surround the C-C bond is considered, [6, 6] bonds can be differentiated in to three types: (i) Pyracylenic or type A, (ii) Type B, and (iii) Pyrenic or type C. The pyracylenic bonds are the shortest bonds and are situated in between two pentagonal rings. They have highest pyramidalization angles and they have a stronger double bond character. The bond that lies in between a hexagon and a pentagon is Type B bond. The type C or pyrenic bond is localized between two hexagonal rings, and it has the lowest piramidalization angles which produces a more planar region of the fullerene structure. Similarly, [5,6] bond can further be classified as: (i) Corannulene or Type D and (ii) Type F. The last bond type is Type E, also known as Pentalene. It is the bond between two pentagons and cannot found in C_{60}.

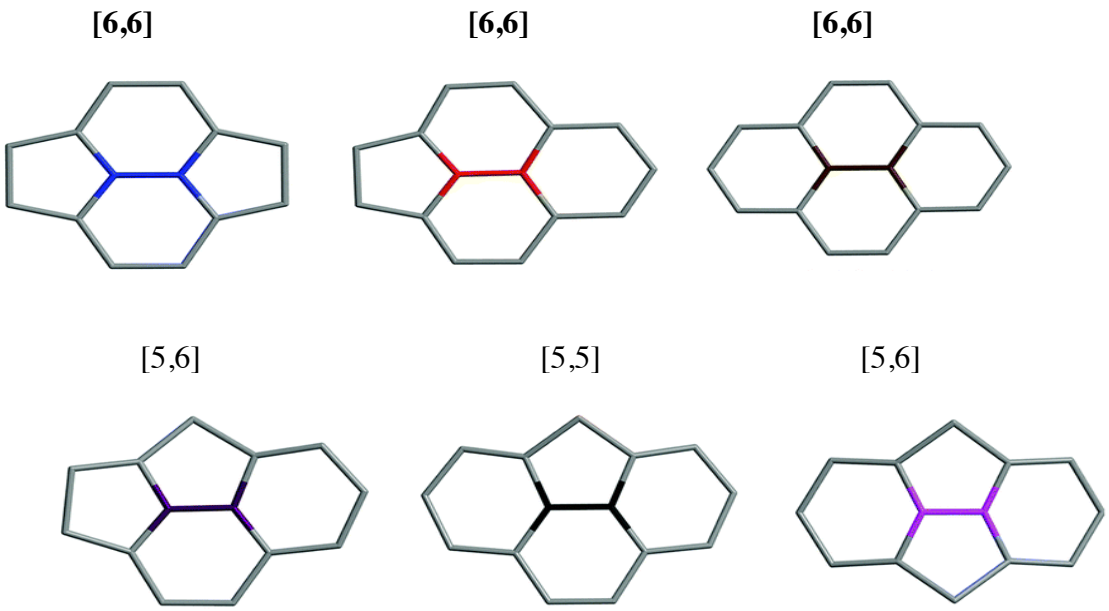

Fig 1.1: Different types of bonds [6, 6], [5, 6] and [5, 5] that might be present in any fullerene.

1.4 The Diels-Alder reaction

It is one of the widely used and versatile reactions that was developed by Professors Otto Diels and Kurt Alder in 1928 [7] and the name of the reaction was after their names. They received Nobel Prize in their work. In the Diels Alder reaction, a conjugated diene reacts with alkene (dienophile) to form a ring. It is the pericyclic reaction meaning it goes on in one step with a cyclic flow of electrons, and involves the addition of a diene molecule to a dienophile. A dienophile molecule is a diene lover. The reaction is in between a molecule with a conjugated π system (the diene) and another with at least one π bond (the dienophile). The [4+2] Diels Alder cycloaddition of 1,3 cis-butadiene is performed easily because of the electron deficient nature of C_{60}. This feature makes C_{60} an ideal dienophile. The [4+2] cycloaddition involves the reaction between 4π electrons of the diene and 2π-electrons of the dienophile. The cycloaddition process proceeds through a cyclic transition state structure breaking the three π bonds of the starting

materials and forming a six membered ring as a product that contain two new sigma bonds and a new π bond. In this process, there is the overlap of the 2p orbitals on carbons 1 and 4 of the diene with the 2p orbitals on the two sp^2 hybridized carbons of the dienophile. These overlaps result two new sigma bonds and a new π bond is formed between carbon 2 and 3 of the diene.

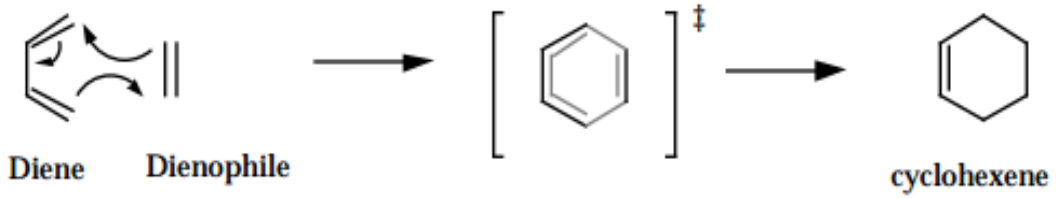

Fig1.2: A Diels-Alder reaction

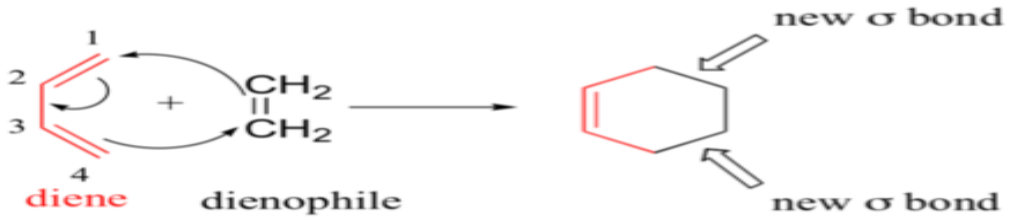

Fig 1.3: An example of Diels-Alder reaction

Dienophile may have two kinds of conformations which are s-cis and s-trans. A *cis* dienophile will produce a ring with *cis* substitution, while a *trans* dienophile will produce a ring

with *trans* substitution. However, in order to occur a Diels-Alder reaction, the diene molecule must have the *s-cis* conformation.

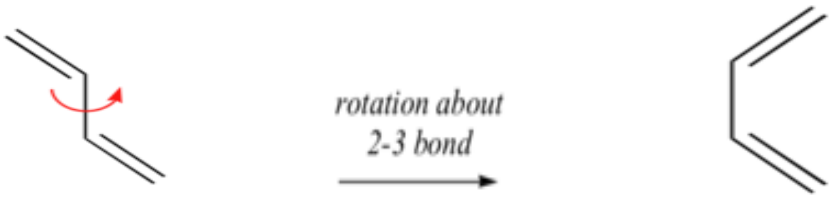

S-trans s-cis

Fig 1.4: Showing the s-trans to s-cis conversion

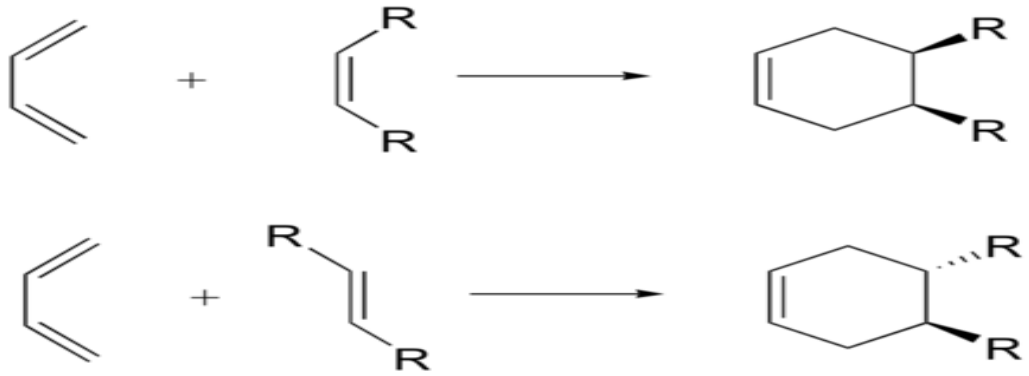

Fig 1.5: Formation of cyclohexene in s-cis and s-trans dienophiles.

1.5 The Exohedral Reactivity

The encapsulated water molecule is expected to modify the exohedral reactivity of the C_{60} cage with respect to the free C_{60}. In order to study the impact of an entrapped water molecule on the chemical reactivity of C_{60}, we studied the thermodynamics and the kinetics of [4+2] Diels-Alder cycloaddition of 1,3-cis-butadiene at all non- equivalent bonds of free C_{60} and H2O@C_{60}.

1.6 Regioselectivity

A reaction is said to be regioselective if one reaction site is preferred over other all possible sites. In our case, it is concerned with which "regions" or "ends" of the diene and dienophile will preferentially react with one another. In the case of C_{60}, cycloaddition reaction is preferred at [6,6] bonds which are shorter and present a larger π density as compared to [5,6].

Chapter 2: Theory

2.1 The density functional theory

Density functional theory is one of the most dominant and successful method to investigate the electronic structure of matter. It is applicable to describe the structural and electronic properties in a large number of materials ranging from atoms and molecules to complex systems. It is computationally simple and has become a common tool to predict the variety of molecular properties such as atomization energies, ionization energies, and vibrational frequencies, electric and magnetic properties and so on. The two core elements of DFT are the Hohenberg-Kohn theorem and the Kohn-Sham equations.

In quantum mechanics a wave function Ψ of a system, at a particular time contains all the information about the system. The Schrodinger equation for an electron moving non relativistically in a potential v(r) can be written as,

$$\frac{-\hbar^2 \nabla^2}{2m} + V(\boldsymbol{r}) = \in \Psi(\boldsymbol{r}) \ .$$

For many body problem,

$$\left[\sum_i^N \left(-\frac{\hbar^2 \nabla^2}{2m} + V(\boldsymbol{r})\right) + \sum_{i<j} U(\boldsymbol{r_i}, \boldsymbol{r_j})\right] \Psi(\boldsymbol{r}_1, \boldsymbol{r}_2, \ldots . \boldsymbol{r}_N) = E\Psi(\boldsymbol{r}_1, \boldsymbol{r}_2, \ldots . \boldsymbol{r}_N) \ , \quad (2)$$

where $U(r_i, r_j)$ the electron - electron interaction and N is the number of electrons.

For a Coulomb interaction,

$$\boldsymbol{U} = \sum_{i<j} U(\boldsymbol{r_i}, \boldsymbol{r_j}) = \sum_{i<j} \frac{q^2}{|\boldsymbol{r_i} - \boldsymbol{r_j}|} \quad (3)$$

For an atom,

$$\boldsymbol{V = \sum_i v(r_i) = \sum_i \frac{Q_q}{|r_i - R|}},$$

where **R** and Q are nuclear position and charge respectively.

For a molecule,

$$\boldsymbol{V = \sum_i v(r_i) = \sum_{ik} \frac{Q_q}{|r_i - R_k|}},$$

where the sum on k is for all nuclei of the system with $Q_k = Z_k e$ and position.

In quantum mechanical approach, the Schrodinger's equation with $v(r)$ can be solved for the wave function Ψ and expectation values of operators with this wave function give rise to observables.

$$v(\boldsymbol{r}) \Longrightarrow \Psi(\boldsymbol{r_1}, \boldsymbol{r_2}, \ldots . \boldsymbol{r_N}) \Longrightarrow \text{Observables.}$$

The observable calculated in this way is the particle density and can be expressed as

$$n(\boldsymbol{r}) = N \int d^3\boldsymbol{r} \int d^3\boldsymbol{r_2} \ldots \ldots \int d^3\boldsymbol{r_N} \ \Psi^*(\boldsymbol{r}, \boldsymbol{r_2}, \ldots . \boldsymbol{r_N}) \Psi(\boldsymbol{r}, \boldsymbol{r_2}, \ldots . \boldsymbol{r_N}).$$

……..(4)

Although there are many powerful methods developed to solve the Schrödinger's equation, density functional theory is more accurate and viable method. It says that knowledge of n(r) implies the knowledge of the wave function and then potential and finally of all other observables. It can be summarized by following way,

$$n(\boldsymbol{r}) \Longrightarrow \Psi(\boldsymbol{r_1}, \boldsymbol{r_2}, \ldots . \boldsymbol{r_N}) \Longrightarrow v(\boldsymbol{r}) .$$

2.1.1 The Hohenberg-Kohn Theorem

The first Hohenberg –Kohn Theorem demonstrates that the electron density uniquely determines the Hamiltonian Operator and thus all the properties of the System. It states that the external potential $V_{ext}(r)$ is a unique functional of $\rho(\boldsymbol{r})$. [8]

Let us consider there are two external potentials $V_{ext}(r)$ and $V'ext(r)$ and each of them giving the same $\rho(\boldsymbol{r})$ for ground state. We will have two different Hamiltonians H and H' with two different normalized wave functions Ψ and Ψ' and same ground state densities.

For Ψ 'as a trial function for Hamiltonian H,

$$E_o < \langle \Psi' | \hat{H} | \Psi' \rangle = \langle \Psi' | \hat{H} | \Psi' \rangle + \langle \Psi' | \hat{H} - \widehat{H'} | \Psi' \rangle = E_o' + \int \rho(\boldsymbol{r}) \, [Vext(r) - V'ext(r)] d\boldsymbol{r},$$

..... (i)

where E_o and E_o' are ground state energies for $\hat{H}$ and $\hat{H}'$ respectively.

Similarly, for Ψ

$$E'_o < \langle \Psi | \hat{H} | \Psi \rangle = \langle \Psi | \hat{H} | \Psi \rangle + \langle \Psi | \hat{H} - \widehat{H'} | \Psi \rangle = E_o + \int \rho(\boldsymbol{r}) \, [Vext(r) - V'ext(r)] d\boldsymbol{r} .$$

..... (ii)

Adding above two equations (i) and (ii) we get, $E_o + E_o' < E_o' + E_o$, which is contradictory result and hence it is not possible to get same $\rho(\boldsymbol{r})$ from two different Vext(**r**).

Therefore, $\rho(\boldsymbol{r})$ determines total number of electrons (N) and electron-nuclear interaction $V_{ext}(r)$ and thus all the properties of the ground state. For example, kinetic energy $T[\rho]$, potential energy $V[\rho]$ and therefore the total energy can be written as,

$$E[\rho] = T[\rho] + V[\rho] + E_{ee}[\rho] = \int \rho(\boldsymbol{r}) \, V_{ne}(r) d\boldsymbol{r} + F_{HK}[\rho],$$

where $F_{HK}[\rho] = T[\rho] + E_{ee}[\rho]$ is known as the holy grail density functional theory and $E_{ee}[\rho]$ is the electron-electron interaction energy.

2.1.2 The Kohn Sham Equations

Kohn and Sham reformulated a genuine approach that the exact ground state density can be written as the ground state density of a system of non-interacting electrons. The ground state charge density for a system of non-interacting electrons is represented as,

$$n(r) = 2 \sum_i |\psi_i(\mathbf{r})|^2,$$

Where i vary from 1 to N/2 for double occupancy of all states and ψ_i(r) is the Kohn- sham orbitals (KS orbitals) and KS orbitals are the solutions of the Schrodinger equation given by,

$$\frac{-\hbar^2 \nabla^2}{2m} + V_{KS}(r) = \in_i \psi_i(\boldsymbol{r}),$$

The KS orbitals ψ_i(r) are not free to be any function. They must obey certain constraints. The electron must be somewhere in space, so the total probability is unity and they are orthogonal. These constraints can be combined as the orthonormality constraints,

$$\int \psi i^*(\boldsymbol{r}) \psi_j(\boldsymbol{r}) dr = \delta_{ij} \qquad (5)$$

2.1.3 The Kohn-Sham Equations and the Variational Principle

A good approach to derive the Kohn Sham equations is the Lagrangian Multipliers method for constrained minimization. To derive the Kohn-Sham equations, one must take the derivative of the functional which is under the concept of calculus of variations. Let us define the constrained functional as,

$E' = E - \sum_{ij} \lambda_{ij} \left(\int \psi_i^* (r) \psi_j(r) dr - \delta_{ij} \right) \ldots\ldots\ldots (6)$, where λ_{ij} are the Lagrange Multipliers.

Under the orthonormality constraints given equation (5) for an arbitrary variation, the variation of E must vanish. That means the functional derivative with respect to ψ_i of the constrained functional given by above equation (6) must be zero.

So, $\frac{\delta E'}{\delta \Psi^*_i(\boldsymbol{r})} = \frac{\delta E'}{\delta \Psi_i(\boldsymbol{r})} = 0$

The energy functional can be rewritten as,

$$E = T_s[n(\mathbf{r})] + E_H[n(\mathbf{r})] + E_{xc}[n(\mathbf{r})] + \int n(\mathbf{r}) V(\mathbf{r}) d\mathbf{r}, \qquad (6)$$

Where the first term is the kinetic energy of *non-interacting* electrons and expressed as,

$$T_s[n(\boldsymbol{r})] = -\frac{\hbar^2}{2m} 2 \sum_i \int \psi_i^*(\boldsymbol{r}) \nabla^2 \psi_i(r) dr$$

The second term is called the Hartree energy and contains the electrostatic interactions between the charges and expressed as,

$$E_H[n(\boldsymbol{r})] = \frac{e^2}{2} \int \frac{n(r) n(\boldsymbol{r}')}{|\boldsymbol{r} - \boldsymbol{r}'|} dr \, dr'$$

The third term is called the *exchange-correlation energy* that contains all the remaining terms. Using the following relation,

$\frac{\delta n(r)}{\delta \psi_i^*(r)} = \psi_i(r) \delta(r - r')$, we get

$$\frac{\delta T_s}{\delta \psi^*_{i(r)}} = -\frac{\hbar^2}{2m} 2 \sum_i \nabla^2 \psi_i(r),$$

$$\frac{\delta E_H}{\delta \psi^*(r)} = e^2 \int \frac{n(r)n(\boldsymbol{r}')}{|\boldsymbol{r}-\boldsymbol{r}'|} dr' \psi_i(r)$$

and combining all above results, we can write,

$$\left(-\frac{\hbar^2}{2m}\boldsymbol{\nabla}^2 + V_H(\boldsymbol{r}) + V_{xc}[n(r)] + V(r)\right)\psi_i(\boldsymbol{r}) = \sum_j \lambda_{ij}\, \psi_j(r) \ldots\ldots\ldots (7),$$

which contains $V_H(r) = e^2 \int \frac{n(r')}{|r-r'|} dr'$, is a Hatree potential

and $V_{xc}[n(r)] = \frac{\delta E_{xc}}{\delta n(r)}$, is an exchange-correlation potential.

The Lagrange multiplier λ_{ij} are obtained from equation (7) and after multiplying it by $\psi_k^*(\mathbf{r})$.

$$\lambda_{ik} = \int \psi_k^*(\mathrm{r})\left(-\frac{\hbar^2}{2m}\nabla^2 + V_H(\boldsymbol{r}) + V_{xc}[n(r)] + V(r)\right)\psi_i(r)dr \qquad (8)$$

2.2 Potential Energy Surface

Potential energy surface (PES) is a complex multidimensional surface and it plays central role in computational chemistry. The non-linear molecule has 3N-6 internal degrees of freedom for the nonlinear molecule while the for the linear molecule has 3N-5 degrees of freedom. Here, N is the number of atoms present in the molecule. The PES is the mathematical or graphical representation of a molecule as a function of the position of atoms or nuclei. The PES facilitates understanding of many useful concepts and allows information intuitive understanding of the energy landscape. The PES arises from the application of the Born Oppenheimer approximation [9] to the solution of the Schrodinger equation. If we consider a general Hamiltonian,

$$H = T_{re} + T_{Rn} + V(r, R) \ldots\ldots\ldots\ldots\ldots\ldots\ldots\ldots\ldots\ldots\ldots (8),$$

where T_{re} is the kinetic energy operator of electronic motion, $T_{Rn}$is the Kinetic energy operator of the nuclear motion, and $V(r,R)$ is the potential energy due to electrostatic interactions of all the electrons and nuclei. According to the BO approximation, the nuclear and electronic degrees of freedom can be separated because the electrons are much lighter than the nuclei so the nuclei are almost at stationary with respect to the electrons. Thus, the nuclear kinetic energy term T_{Rn} can be neglected in above equation. Then, the time dependent Schrodinger equation for the electronic degrees of freedom is expressed as,

$$[T_{re} + V(r,R)]\Phi(r,R) = E(R)\,\Phi(r,R) \ldots\ldots\ldots\ldots\ldots\ldots\ldots\ldots\ldots (9)\ ,$$

where $E(R)$ is a function of nuclear degrees of freedom and $\Phi(r,R)$ is the electronic wave function. The potential energy surface is the plot of $E(R)$ vs $\Phi(r,R)$as shown in figure below. A reaction on the potential energy surface is a path walking from the valley of the reactants to the valley of the products. Thus, one must be able to find the minima, transition states and higher order saddle points on the potential energy surface.

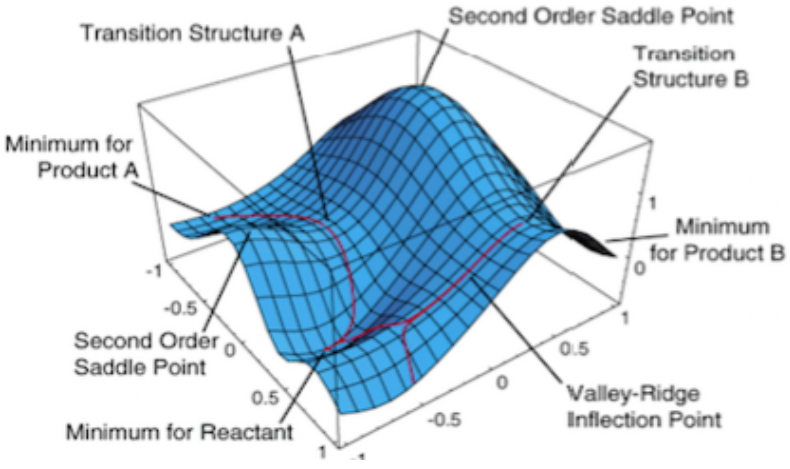

Fig 2.1: A model of energy surface (From H. B. Schlegel, Wayne State University)

2.3 Transition States

An intermediate configuration on the reaction path between the initial and final arrangements of atoms or molecules is known as the Transition State. The energy difference between the transition state and the initial state is referred to as the activation energy of that reaction. It is the minimum energy required to acquire the reaction and it has always positive value. The energy of transition state is always higher than the reactants and products independent of if the reaction is endergonic or exergonic. Thus, it is the least stable state.

$$Activation\ energy = Transition\ state\ energy - energy\ of\ reactants$$

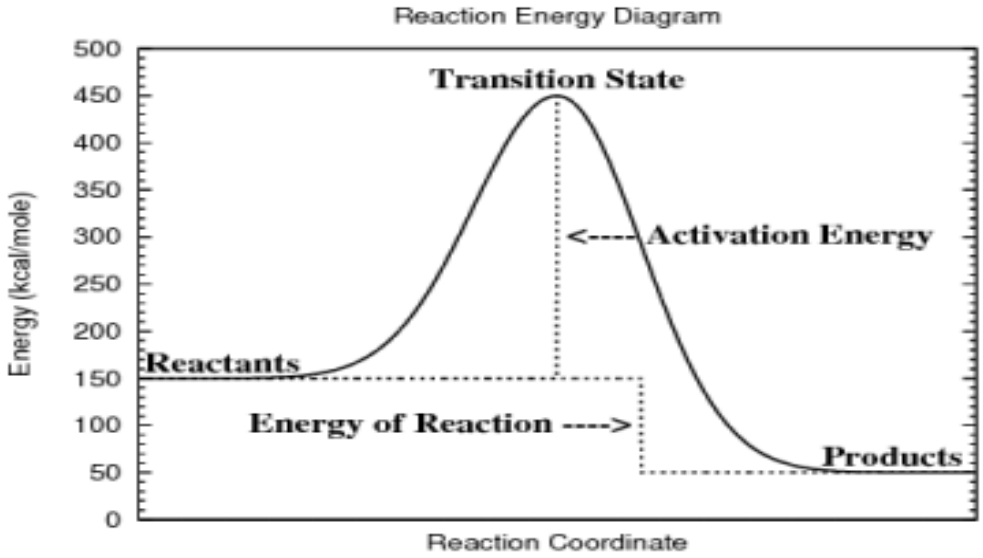

Fig 2.2: Figure showing the reaction path

2.4 Transition States on Potential Energy Surface

Transition state is a saddle point on the energy surface which has maximum energy along the reaction path and minimum energy along the directions perpendicular to the reaction path. It is necessary to locate the first order saddle points on the potential energy surface to get the

reaction barriers and the reaction rates. Finding the transition state (TS) on a potential energy surface is the important work for the reaction mechanism. The equilibrium geometry of a molecule represents the minimum in the potential energy surface. The first derivative of the PES corresponds to the gradient while the negative gradient of PES is the force. The first derivative is not sufficient to say anything about the minimum, a transition state and higher order saddle point. Thus it is necessary to check to the second derivative. The PES has minimum value if it's second derivative is positive and maximum value if it's second derivative is negative. The matrix of second derivatives of the potential energy surface is known as the Hessian matrix. The Hessian matrix with its mass weighted coordinates and is diagonalized to obtain eigenvectors and eigenvalues. The eigenvectors are the normal modes of the vibrations and eigenvalues are proportional to the square of the vibrational frequencies.

The gradient vector or first derivative vector and the Hessian matrix or second derivative matrix with respect to molecular coordinates $\boldsymbol{R}$ are expressed as follows:

$$G_i = \frac{\partial E}{\partial R_i} \qquad \text{and } H_{ij} = \frac{\partial 2E}{\partial R_i \partial R_j} \ .$$

Hessian can be diagonalized by using a unitary matrix U as $HU = Uh$

And then in new coordinates it can be written as,

$$U^t H U = h = \begin{pmatrix} h_1 & \cdots & 0 \\ \vdots & \ddots & \vdots \\ 0 & \cdots & h_n \end{pmatrix} \qquad (h_1 < h_2 < \quad \ldots\ldots < h_n)$$

2.5 Transition states Optimizations

The quality of the starting structure provided by the user for geometry minimization as well as optimization, the choice of coordinate system, algorithm choice, initial Hessian and quality of the updated Hessian play important role for the success and efficiency of a calculation.

There are several methods used for the geometry minimizations such as (i) Newton Methods (ii) The geometry optimization by direct inversion of the iterative subspace, or GDIIS method (iii) Conjugate gradient and LBGIS method, and (iv) algorithms designed to find surface intersections and points of closest approach.

Similarly, for the transition state optimization, (i) local methods (ii) Climbing, bracketing, and interpolation methods (iii) path optimization methods, are frequently used. One of the most often used method to determine the starting structure for the search of the transition states is the calculation on one dimensional slice of the potential energy surface; that is, potential energy curve. The idea is that out of all the internal degrees of freedom of the molecule (3N-6, where N is the number of atoms, 3 rotational and 3 translational coordinates are removed), there is one coordinate that determines the transition from reactants to products. Then, we do the constrained optimization by varying this coordinate and then optimizing all other variables while keeping it fixed; and find the maximum along the calculated path which corresponds to the Transition State.

The following figure is the one dimensional potential energy surface for a reaction. Thick line is the energy curve and the curves 1, 2 and 3 are the quadratic curves approximating locally the energy curve around the three stationary points.

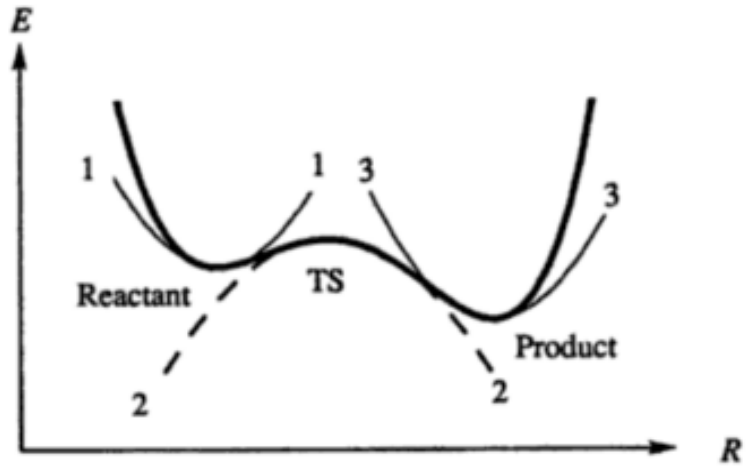

Fig 2.3: One dimensional slice of potential energy curve

For both the transition state and the minimum $\frac{\partial E}{\partial R} = 0$ and at the transition state, $\frac{\partial 2E}{\partial R^2} < 0$ along the reaction coordinate and, $\frac{\partial 2E}{\partial R^2} > 0$ for all coordinate except the reaction coordinate.

2.6 Verification of Transition States

It is necessary to verify the transition structures after the TS optimization. Basically, there are two steps to verify TS. At first, the Hessian must be evaluated and diagonalized for that structure to confirm that it has one, and only one negative eigenvalue. The second step is to test whether the saddle point lies on the way of path of reaction when moving from reactant to product minima. This can be done by employing the reactant path following or visualizing the displacement along the vibrational mode corresponding to the imaginary frequency or both. If any of the structures do not complete these two steps, the optimization structure is not valid.

Chapter 3: Results and Discussion

In order to obtain the stable geometry of H2O@C60 we started with several different configurations in which H2O molecule was placed inside the C60 cavity with different orientation. In total 12 isomers were generated. All isomers were optimized using the DFT the forces on each atom was beyond the threshold 10^{-4}. The dispersion interaction were included using the Grimme's DFT-D3 semi-empirical approach. The DFT-D3 computation of forces is post convergence. Therefore it's impact on the electronic structure of the system is indirect, that is, only through the changes in the geometry. The total energies of the optimized isomers were essentially identical within numerical thresholds which indicate that the water molecule may be rotating inside the cavity. To investigate the mobility of water molecule in C60, we performed a molecular dynamics simulation with density functional interatomic potential for 2 ps. The visualization of molecular dynamics trajectories show that the water molecule rotates inside the C60. We also examined the vibrational stability of the H2O@C60. The infra-red and Raman spectra are shown in Figure. 3.1.

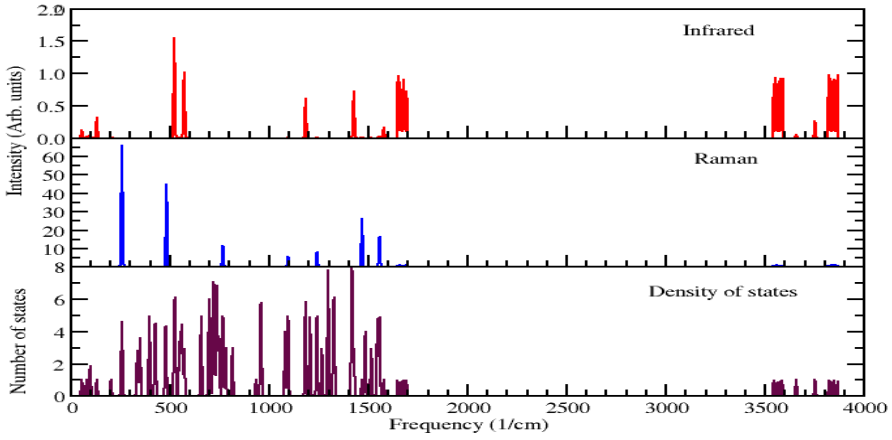

Fig 3.1: The infrared Raman Spectra, vibrational density of states of $H_2O@C_{60}$

The infra-red spectra agree with the experimental spectra. The polarizability of the H2O@C60 is 83 $Å^3$ very slightly different from that of C60 (82 $Å^3$). The endohedral water molecule has essentially no impact on the polarizability of H2O@C60. The vibrational contribution to the polarizability however increases from 0.6 $Å^3$to 4.26 $Å^3$.

To gauge the accuracy of our computational model for the study of Diels-Alder reaction between 1, 3 cis-butadiene and $H_2O@C_{60}$, we first computed the examined the reaction with C_{60}. The Diels-Alder reaction between 1, 3 cis-butadiene and all the nonequivalent bonds of C60 fullerene has been thoroughly studied. For the C_{60} fullerene with its icosahedral symmetry, only two types of nonequivalent bonds are possible: pyracylenic bonds (a type A [6, 6] ring junction) and corannulenic bonds (a type D [5, 6] junction). We also considered the [6, 5] bond for the reaction, which is basically same as [5, 6] but shows the orientation of the molecule. The reaction energy of [6,6] bond of free C_{60} is -1.46 eV. Similarly, for [5, 6] and [6, 5] are -0.69 eV and -0.70 eV. It shows that [5,6] or [6, 5] bonds are clearly less favorable for cycloaddition. This conclusion is in agreement with literature results however there is difference in absolute values of the energies. The energies predicted by our model are larger compared to the literature. We expect however that our model will correctly predicts the trends.

Bearing this in mind, we studied the Diels-Alder reaction between 1,3 cis butadiene and $H_2O@C_{60}$ at all nonequivalent bonds of C_{60} cage. We know that exohedral reactivity of C_{60} occurs mainly at the [6,6] bonds [11,12]. However, we analyzed the thermodynamics and kinetics of the reaction for all non-identical bonds [6,6], [5,6] and [6,5] bonds. The table 1 lists the reaction energies for all bonds we have studied. The reaction energies for [6,6], [5,6] and [6,5] are -1.47, -0.71 and -0.72 respectively for H2O@C60. Also, the reaction energies for free C_{60} are -1.46, -0.69 and -0.70 for respective bonds as shown. The comparison of reactivities of

bare C_{60} and $H_2O@C_{60}$ shows that like in bare in C_{60} fullerene, the reaction is still more exothermic at [6,6] bonds. Thus, the reactivity of free C_{60} is not affected significantly by encapsulation of a water molecule. The result that encapsulation of water has no bearing on the reactivity of C_{60} is somewhat unexpected as water due to its polar nature is expected to introduce changes in the charge distribution. In fact, the water encapsulation does result in a small dipole moment (0.48 Debye) which is an evidence of changes in the electron distribution in the $H_2O@C_{60}$. As mentioned earlier these changes also results in somewhat larger value of vibrational polarizability of $H_2O@C_{60}$. Oguna and coworkers have studied the reactivities of noble atom and their dimers encapsulated in C_{60}. Their results show that the reactivity of C_{60} encapsulating a single noble atoms did not differ from that of pure C_{60}. Likewise, the encapsulation of dimers of lighter noble atoms in C_{60} made insignificant impact on the reactivity of the endohedral complexes. In all these cases, the cycloaddition was favored over [6,6] bond than over [5,6] bond. This situation however is changed for the C_{60} containing heavier noble dimers. In this case it was found their encapsulation increased the reaction under both thermodynamic and kinetic control. The changes were particularly pronounced for the $Xe_2@C_{60}$ where addition to [5,6] and [6,6] both became equally viable. These difference was attributed to stabilization of LUMO and to the strain energy of the fullerene. In the present $H_2O@C_{60}$ the geometrical changes in the fullerene shell, like in light noble atoms (dimers) encapsulated C60, are negligible (0.2 eV). These results seem to indicate that the strain in the fullerene shell, rather than the changes in the electronic distribution, are responsible for changes in the reactivity.

Table 3.1: Reaction Energies for [6, 6], [5, 6] and [6, 5] bonds of $H_2O@C_{60}$ and C_{60}.

Bond types	DE for H2O@C60 (eV)	DE for C60 (eV)
[6,6]	-1.47	-1.46
[5,6]	-0.71	-0.69
[6,5]	-0.72	-0.70

More importantly, the optimized products after the addition of 1, 3 cis-butadiene on free C_{60} and $H_2O@C_{60}$ look similar. The C-C bond length of the products 'Rcc' is 1.57A at [6, 6] for both C_{60} and $H_2O@C_{60}$. Also, the final Rcc values of the products for the addition to [5,6] and [6, 5] bonds of $H_2O@C_{60}$ and C_{60} are same.

Table 3.2: C-C bond lengths for $H_2O@C_{60}$ and C_{60} at [6, 6], [6, 5] and [5, 6] of optimized products.

Bond Types	Rcc for $H_2O@C_{60}$(Å)	Rcc for C_{60}(Å)
[6,6]	1.57	1.57
[5,6]	1.57	1.57
[6,5]	1.57	1.57

We also calculated the activation barriers for $H_2O@C_{60}$ and free C_{60}. The following table shows the activation barriers for all studied bonds.

Table 3.4: Activation barriers for [6, 6], [6, 5] and [5, 6] of $H_2O@C_{60}$ and C60

Bond Types	Eact (eV) ($H_2O@C_{60}$)	Eact (eV) (C_{60})
[6,6]	0.37	0.38
[6,5]	0.56	0.58
[5,6]	0.62	0.65

As shown in the table, the activation barrier for the [6,6] bond of $H_2O@C_{60}$ is 0.37 eV, which is very close the value 0.38 A for C60. Similarly, we located the transition states at [5,6] and [6,5]. The activation barriers for [5,6] and [6,5] are 0.56 and 0.62 which are close to the values of C_{60} obtained as 0.58 and 0.65 respectively. From the transition states geometries, it observed that, the bond lengths that are being formed R_{cc} are approximately the same as observed in C_{60}. The bond lengths for $H_2O@C_{60}$ and C_{60} at [6,6] is 2.3 A. Similarly, for the bonds [5,6] and [6,5], the C-C bond lengths are 2.7 A and 2.6 A respectively, which are close to the values obtained for free C_{60}.

Table 3.5: C-C bond lengths for $H_2O@C_{60}$ and C_{60} at [6,6], [6,5] and [5,6] of transition states.

Bond types	Rcc^+ for $H_2O@C_{60}$	Rcc^+ for C_{60}
[6,6]	2.3	2.3
[5,6]	2.6	2.7
[6.5]	2.7	2.6

Table 3.3: Showing all activation energies for all isomers.

Isomers	R_{cc} (Å)	E_{act} (eV)	Rings	
1	2.6	0.63	5	6
2	2.3	0.37	6	6
3	2.7	0.63	5	6
4	2.4	0.37	6	6
5	2.6	0.56	6	5
6	2.3	0.37	6	6
7	2.7	0.62	5	6
8	2.7	0.56	6	5
9	2.7	0.56	6	5
10	2.7	0.63	5	6
11	2.3	0.38	6	6
12	2.7	0.65	5	6
13	2.3	0.38	6	6
14	2.7	0.57	6	5
15	2.3	0.37	6	6
16	2.7	0.62	5	6
17	2.6	0.56	6	5
18	2.6	0.56	6	5

We also analyzed the charge distribution on fullerene cages. The following table shows the distribution of charges.

Table 3.6: Charge distribution at when a polar water molecule is inside the cage.

Charge on Isomers	$H_2O@C_{60}$-C_4H_6	H_2O	C_4H_6	$H_2O@C_{60}$	C_{60}	Rings
1	0	-0.02	0.121	-0.121	-0.119	5 6
2	0	-0.02	0.117	-0.117	-0.115	6 6
3	0	-0.02	0.117	-0.117	-0.115	5 6
4	0	-0.01	0.12	-0.12	-0.119	6 6
5	0	-0.01	0.115	-0.115	-0.114	6 5
6	0	-0.01	0.119	-0.119	-0.118	6 6
7	0	-0.02	0.119	-0.119	-0.114	5 6
8	0	-0.02	0.116	-0.116	-0.114	6 5
9	0	-0.02	0.116	-0.116	-0.118	6 5
10	0	-0.02	0.12	-0.12	-0.118	5 6
11	0	-0.02	0.119	-0.119	-0.117	6 6
12	0	-0.02	0.118	-0.118	-0.116	5 6
13	0	-0.02	0.117	-0.117	-0.115	6 6
14	0	-0.02	0.114	-0.114	-0.112	6 5
15	0	-0.02	0.118	-0.118	-0.116	6 6
16	0	-0.01	0.118	-0.118	-0.117	5 6

17	0	-0.01	0.116	-0.116	-0.115	6 5
18	0	-0.02	0.114	-0.114	-0.112	6 5

Table 3.7: Charge distribution when a water molecule is taken out of the cage.

Charge on Isomers	C_4H_6	C_{60}	Bond type
1	-0.155	1.155	[6,6]
2	-0.151	1.151	[6,5]
3	-0.162	1.162	[5,6]

Therefore, it is found that entrapment of a polar water molecule though perturbs the charge distribution on the host C_{60}, does not significantly affect the exohedral reactivity of C_{60}.This is due to mainly due to the fact that H_2O molecule inside the hydrophobic environment environment is electrochemically stable [10]. Cycloaddition is greatly favored at [6, 6] bond because it is symmetric in nature and shorter in lengths in comparison with other bonds [5, 6] and [6,5] and larger π electron density.

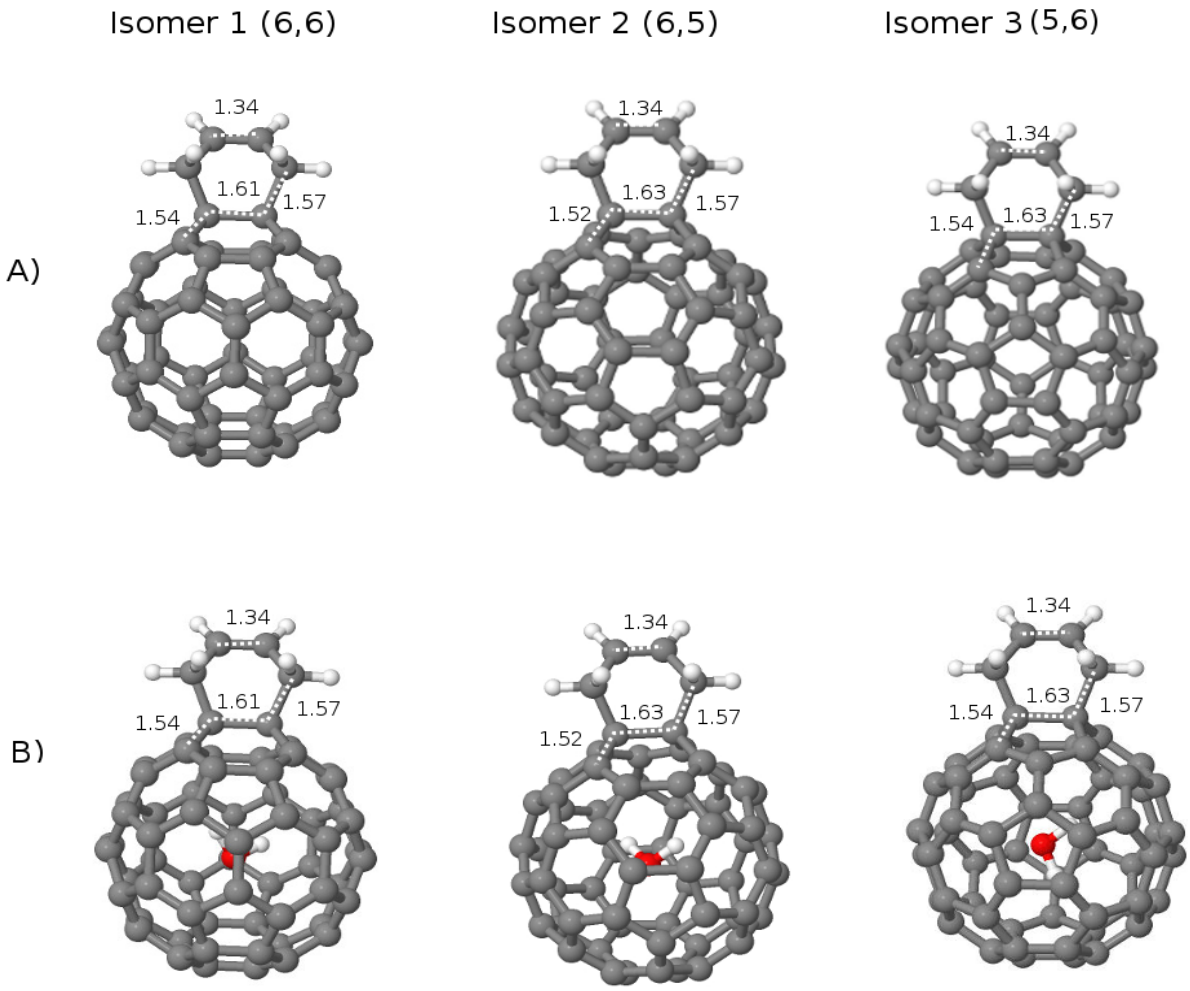

Fig 3.2 : Bond lengths measured at [6,6], [6,5] and [5,6] of optimized products

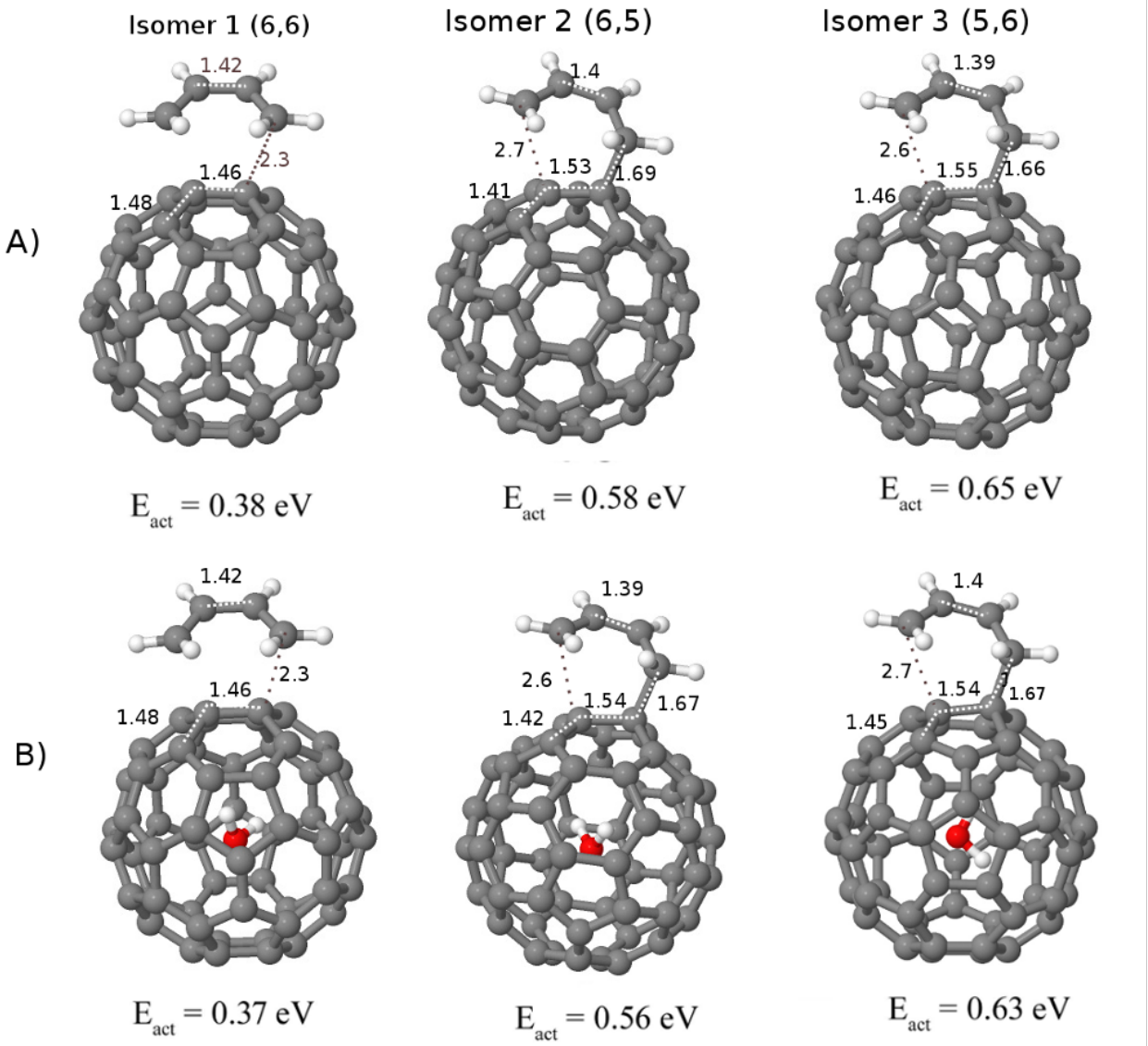

Fig 3.3: Bond lengths for [6,6], [6,5] and [5,6] for C_{60} and $H_2O@C_{60}$ at transition states.

.

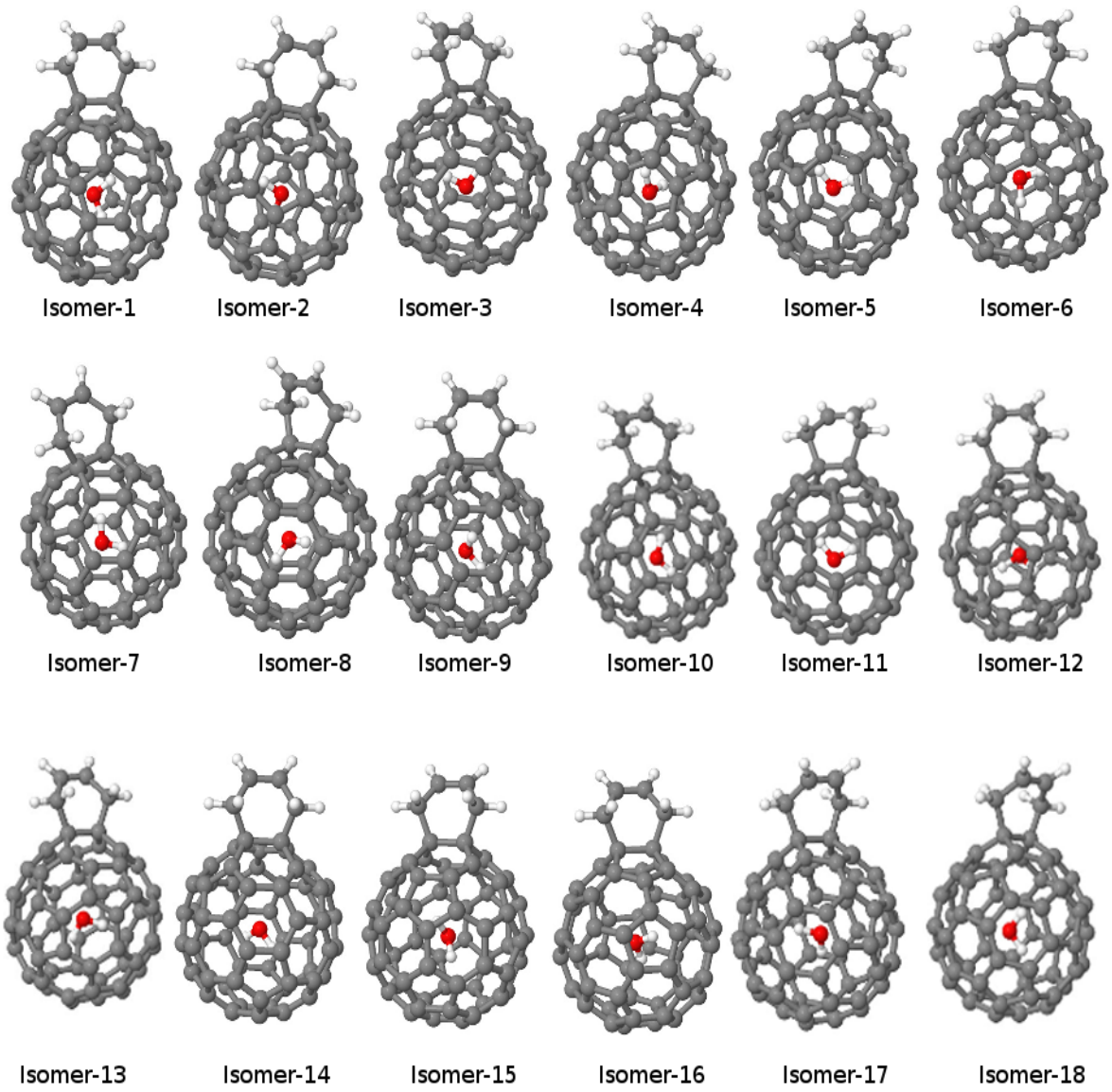

Fig 3.4: Optimized figures of all the isomers.

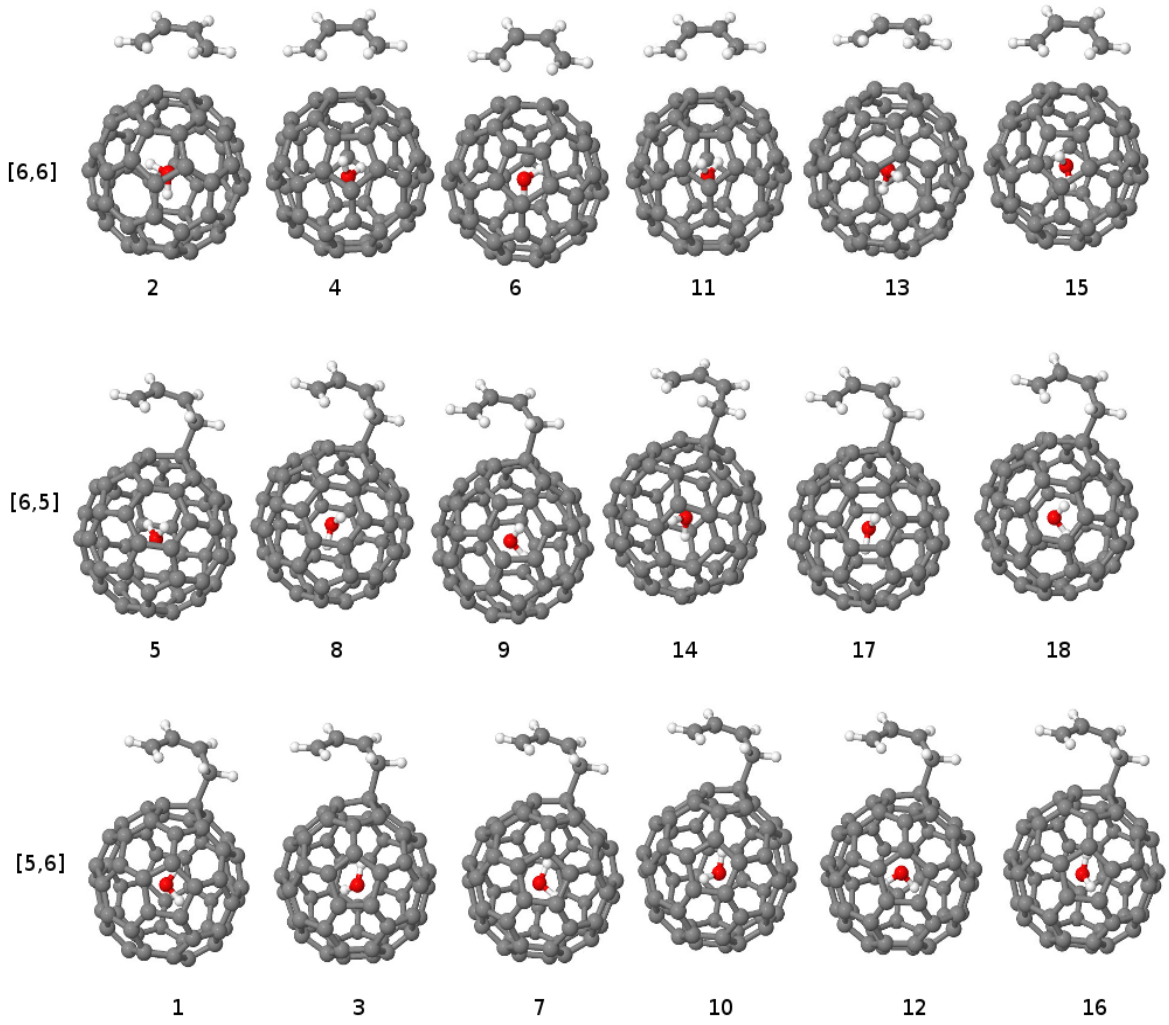

Fig 3.5: Transition state figures of all the isomers

Chapter 4: Conclusions

We have studied the [4+2] Diels- Alder reaction of the $H_2O@C_{60}$ with an organic compound 1, 3 cis-butadiene. The study was performed from both thermodynamics and kinetic points of view. The study of reactions of $H_2O@C_{60}$ showed that encapsulation of a single water molecule does not affect significantly on the exhodedral reactivity of C_{60}. The cycloaddition is clearly favored at [6, 6] bonds.

References

1. Noh, Tae Hwan, et al. "Motion of an isolated water molecule within a flexible coordination cage: structural properties and catalytic effects of ionic palladium (II) complexes." Journal of the American Chemical Society 133.5 (2011): 1236-1239.
2. K. Kurotobi, Y. Murata, Science 2011, 333, 613 – 616.
3. Osuna, Sílvia, Marcel Swart, and Miquel Solà. "Reactivity and Regioselectivity of Noble Gas Endohedral Fullerenes Ng@C_{60} and Ng_2@C_{60} (Ng= He–Xe)." Chemistry–A European Journal 15.47 (2009): 13111-13123.
4. J. R. Heath, S. C. Obrien, Q. Zhang, Y. Liu, R. F. Curl, H. W. Kroto, F. K. Tittel, R. E. Smalley, J. Am. Chem. Soc. 1985, 107, 7779 – 7780; H. W. Kroto, J. R. Heath, S. C. Obrien, R. F. Curl, R. E. Smalley, Nature 1985, 318, 162 – 163.
5. https://en.wikipedia.org/wiki/Endohedral_fullerene.
6. Gao, Yuan, and Baoxing Xu. "Probing Thermal Conductivity of Fullerene C60 Hosting a Single Water Molecule." The Journal of Physical Chemistry *C*119.35 (2015): 20466-20473.
7. Diels, O; Alder, K. Ann. 192*8,* 460, 98.
8. Juan Carlos Cuevas, Introduction to Density Functional Theory. Retrieved from https://www.uam.es/personal_pdi/ciencias/jcuevas/Talks/JC-Cuevas-DFT.pdf
9. https://en.wikipedia.org/wiki/Born%E2%80%93Oppenheimer_approximation
10. K. Kurotobi, Y. Murata, Science 2011, 333, 613 – 616.
11. R. Taylor, D.R. Walton, Nature 1993, 363, 685–693; A. Hirsch, Angew. Chem. 1993, 105, 1189 – 1192; Angew. Chem. Int. Ed. Engl. 1993, 32, 1138 – 1141; A. Hirsch, The Chemistry of

Fullerenes, Thieme, Sttutgart, 1994 ; W. S ´ liwa, Fullerene Sci. Technol. 1995, 3, 243 – 281; W. S ´ liwa, Fullerene Sci. Technol. 1997, 5, 1133 – 1175.

12. M. Solà, J. Mestres, J. Martí, M. Duran, Chem. Phys. Lett. 1994, 231, 325 – 330 ; A. Chikama, H. Fueno, H. Fujimoto, J. Phys. Chem. 1995, 99, 8541 – 8549.

Vita

Govinda KC was born in Nepal. He completed his Masters of Science from Tribhuvan University, Neapl. He Joined the University of Texas at El Paso in August, 2014 as a graduate student. He got the opportunity to work as a teaching assistant in the Department of Physics at University of Texas at El Paso.

Permanent address: Lung-6, Bahane, Pyuthan, Nepal

This thesis/dissertation was typed by Govinda KC.